Article ID: 1003－6326(2004)02－0340－05

Cell-structure and mechanical properties of closed-cell aluminum foam①

ZHOU Yun(周 芸)[1], ZUO Xiao-qing(左孝青)[1], SUN Jia-lin(孙加林)[1], S. R. Nutt[2]
(1. Department of Materials Engineering, Kunming University of Science and Technology, Kunming 650093, China;
2. Materials Science Department, University of Southern California, Los Angeles, CA 90089-0241, USA)

Abstract: The density, cell size and structure of closed-cell aluminum foam were measured by optical microscopy and image analysis. The properties and the mechanism of compressive deformation that occur in closed-cell aluminum foam were measured and discussed. The results show that the cell size of foam with density of 0.37 mg/m^3 is distributed in the range of 0.5－4.0 mm. The cell size of foam with density of 0.33 mg/m^3 is distributed in the range of 0.5－5.0 mm. The cell wall thickness of both types is 0.1－0.3 mm. The closed-cell aluminum foam almost belongs to isotropic one, with a variation of ±15% in elastic modulus and yield strength in longitudinal and transverse direction. Under compressive loading, foam materials show inhomogeneous macroscopic deformation. The site of the onset of local plastic deformation depends on the cell structure. The shape of cell is more important than size in determining the yielding susceptibility of the cells. At early stage of deformation, the deformation is localized in narrow bands having width of one cell's diameter, and outside the bands the cell still remains the original shape. The cells within bands experience large permanent deformation. The band normals are usually within 20° of the loading axis.

Key words: aluminum foam; cell structure; mechanical properties
CLC number: TB 383; TF 125.6 **Document code:** A

1 INTRODUCTION

Metal foams exhibit unusual mechanical, thermal, acoustic, damping, electrical and chemical properties that cannot be found in solid materials. Those special properties may lead to a variety of applications in structural and functional products. Closed-cell aluminum foam is a light-mass structural material of great promise. Its density is only a fraction of that of the corresponding bulk metal, but its strength is sufficiently high to be used in the automobile industry, building industry and transportation. Examples of their applications include panels for vehicles, building and transport; non-flammable ceiling and wall panels for thermal and sound insulation. For successful design with this new material, it is important to determine its structural characteristics and properties[1-9].

The closed-cell aluminum foam board was manufactured by melt foaming method. In this paper, the structural characteristics of closed-cell aluminum foam board were provided. Also, compressive properties were measured in the Instron 8500 machine in displacement control at a rate of 1.5 mm/min. Surface strain mapping was used to determine and analyze the cell deformation behavior and mechanisms.

2 MATERIAL CHARACTERISTICS

2.1 Material density

The average density of sample investigated is listed in Table 1. The samples were cut from a 300 mm × 300 mm × 20 mm board of aluminum foams produced by direct metal foaming. The dimension of samples is 25 mm × 25 mm × 20 mm. The distribution of the apparent density along the width direction of board is shown in Fig. 1. The apparent

Table 1 Average densities of foam sample

Sample No.	Relative density	Density/(mg·m^{-3})
1	0.148	0.40
2	0.125	0.34
3	0.130	0.35
4	0.135	0.37
5	0.139	0.38
6	0.138	0.37
7	0.137	0.37
8	0.135	0.36
9	0.128	0.34
10	0.135	0.36
11	0.149	0.40

① **Received date:** 2003－07－09; **Accepted date:** 2003－10－16
Correspondence: ZHOU Yun, Associate professor; E-mail: zyuncrystal@yahoo.com

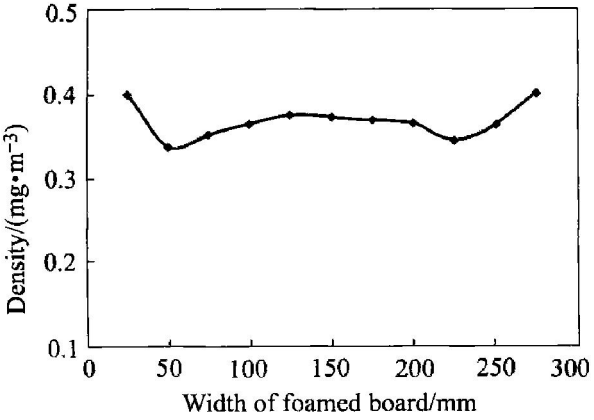

Fig. 1 Distribution of apparent density along width direction of foamed block

density is high at each side of the board, but gradually decreases then slowly increases toward the center of the board. The reason is that the cooling speed is different in different parts of the board.

2.2 Cell morphology

The typical cell structures on polished cross-sections are shown in Fig. 2. It can be seen that the foam materials contain heterogeneities and imperfections in their structures. The cell size is distributed in the range of 0.5 – 4.0 mm with a mean cell size of 2.2 mm(Fig. 3(a)). For the foam with density of 0.33 mg/m^3, its mean cell size is 2.5 mm(Fig. 3(b)) and the cell size is distributed in the range of 0.5 – 5.0 mm. The cell size of foam with density of 0.37 mg/m^3 are smaller than that with density of 0.33 mg/m^3. The cell wall thickness of both types is between 0.1 mm and 0.3 mm.

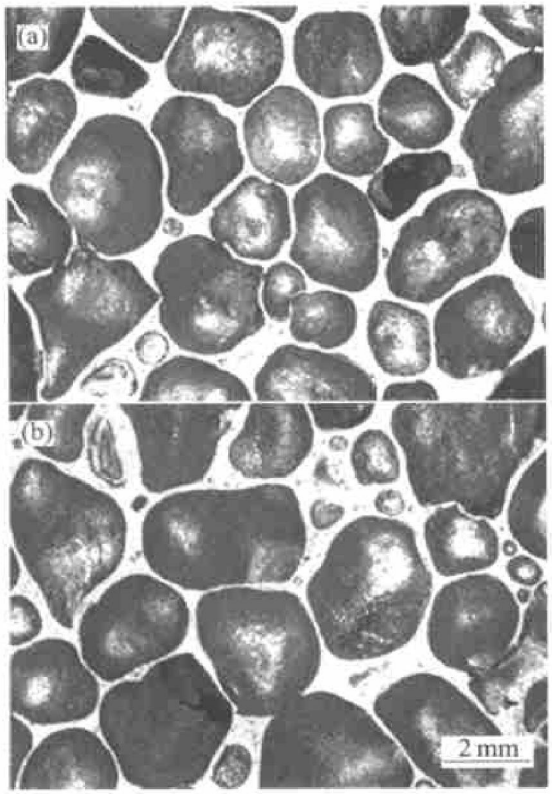

Fig. 2 Typical cell structure morphologies of foams with different densities
(a) —0.37 mg/m^3; (b) —0.33 mg/m^3

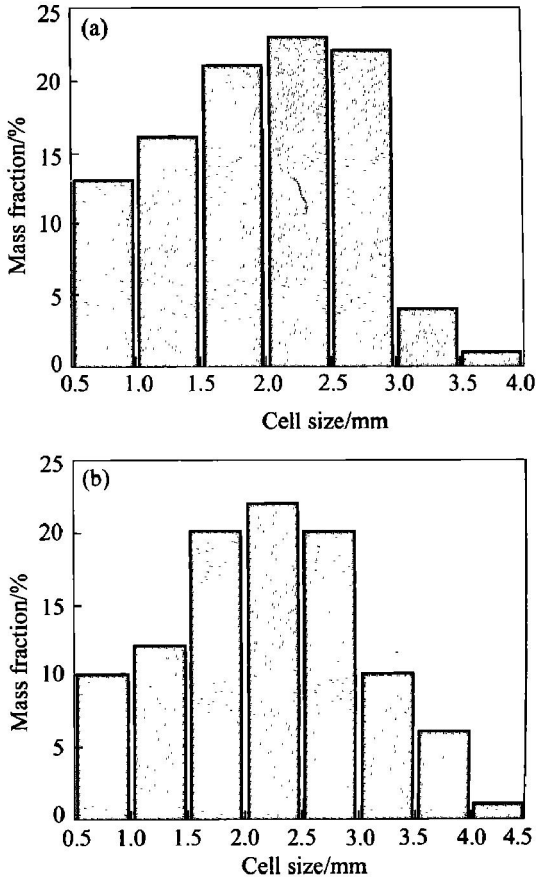

Fig. 3 Cell size distribution of foams with different densities
(a) —0.37 mg/m^3; (b) —0.33 mg/m^3

3 MECHANICAL BEHAVIOUR

3.1 Compressive response

Compression tests of the foam materials at room temperature were conducted. The elastic modulus was measured by loading the foam sample into the plastic range, then unloading and determining the modulus from the unloading slope[10]. The average values of measured mechanical properties of the foam are listed in Table 2. Typical compressive stress — strain curves for longitudinal(parallel to the foam expansion direction) samples and transverse(perpendicular to the foam expansion direction) samples are presented in Fig. 4.

The data of compression test in Table 2 and the compression curve in Fig. 4 show that the

Table 2 Compression properties of aluminum foam

Direction	Relative density	Density/(mg·m^{-3})	Elastic modulus/GPa	Compression strength/MPa
Longitudinal	0.134	0.362	1.35	4.41
Transverse	0.133	0.359	1.30	3.87

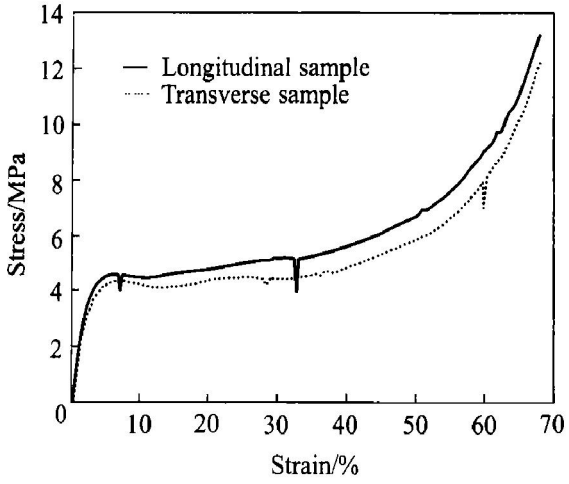

Fig. 4 Compressive stress—strain curve of aluminum foam

closed-cell aluminum foam is almost isotropic, with a variation of ±15% in elastic modulus and yield strength between longitudinal and transverse samples. Olurin[11] considered that a foam is isotropic, with modulus and yield strength varying with specimen orientation by ±15%. Both curves show a local peak stress at yield stage, followed by a fairly constant plateau stress.

3.2 Evolution of deformation

The evolution of deformation of cell structures in compressive test is shown in Fig. 5. It is found that strain distribution is locally non-uniform, even at small strain rate. The site of the onset of local plastic deformation depends on the cell structure. Some investigation with X-ray CT images reveal that there is no obvious preference for the larger cells to be more susceptible to plastic deformations[12]. That is to say, large cells remain elastic provides that they have equiaxial morphology with minimal ellipticity. The implication is that shape is more important than size in determining the yielding susceptibility of the cells.

It can be seen that at strain below 10%, deformation is mainly concentrated in a plane of cells close to the upper surface of sample(Fig. 5). However, deformation was not confined to this region. It can be seen that the cells subsequently deformed in bend and twist with the increase of strain, As deformation progress, co-operative collapse occurs, forming both an inclined and an approximately horizontal band of localized deformation[13]. It is clear that an interaction among cells is necessary for deformation to proceed within narrow bands. Typically, at the load below the peak stress ($\sigma/\sigma_p = 0.3$), a band having width about one-cell diameter(2 ~ 3 mm) initiates, then the band propagates across the specimen as the load increases. At the stress peak, the band extends across the entire specimen with local densification.

The deformation mode of three typical cells during compression was represented by Bart-Smith et al[12]. The displacements of the cell walls before and after straining are presented in Fig. 6. The cells outside the deformation bands deform elastically and retain their original shapes(Fig. 6(a)). Conversely, the cells within the bands manifest permanent plastic deformations(Figs. 6(b) and (c)).

3.3 Surface strain mapping

Surface stain analysis is carried out by using commercial surface displacement analysis(SDA) software, which performs an image correlation analysis by comparing pairs of digital images captured during the loading. The images are divided

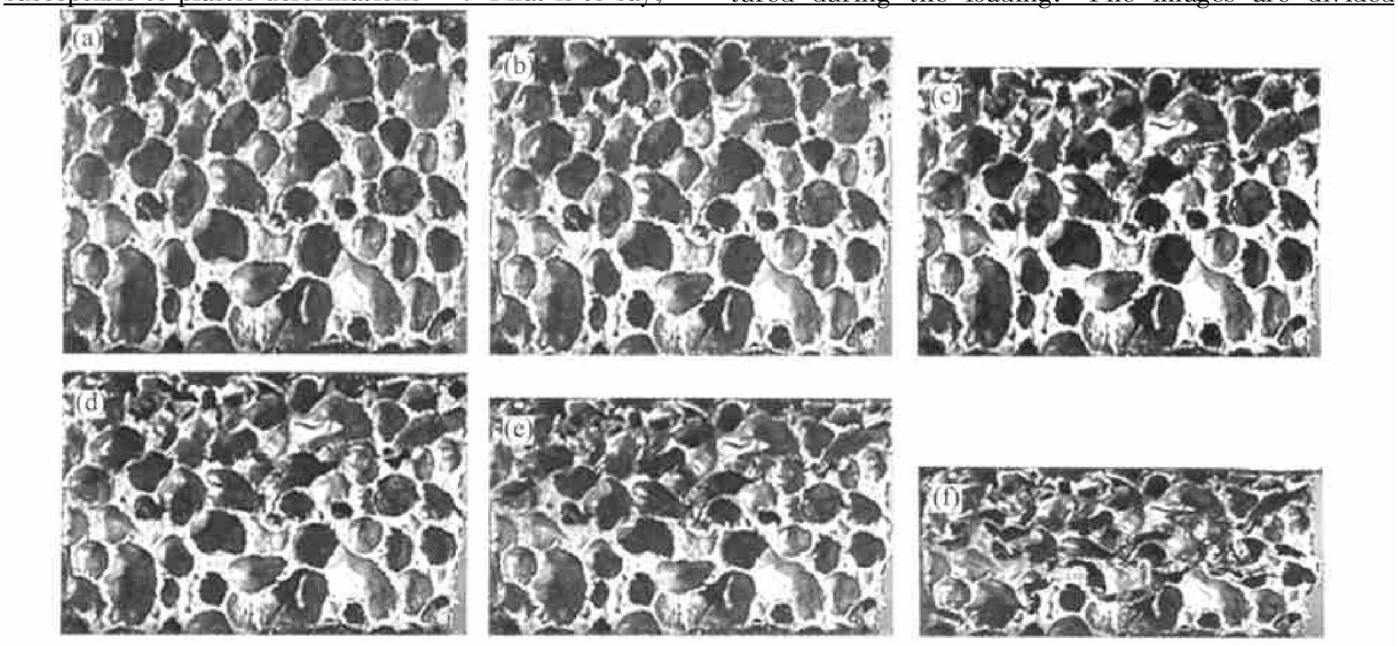

Fig. 5 Evolution of deformation during compression of aluminum foam
(a) —0% deformed; (b) —10% deformed; (c) —20% deformed; (d) —30% deformed; (e) —40% deformed; (d) —50% deformed

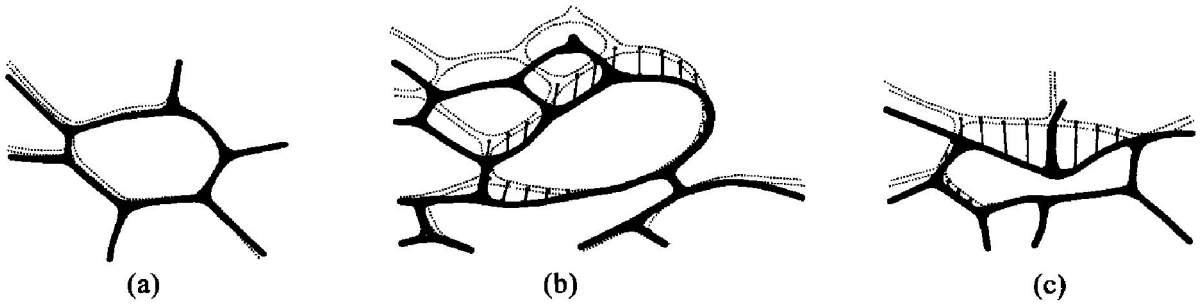

Fig. 6 Schematics of three typical cells before and after 5% strain
(a) —A cell that experiences minimal change; (b) and (c) —Cells within deformation bands that experience appreciable permanent deformation

into sub-images, which provide an array of analysis sites on the surface. Displacement vectors from these sites are evaluated through a series of 2D-fast fourier transform (FFT) calculations of corresponding pairs of sub-images. Surface images were recorded using commercial video camera with a CCD array of 640 × 480 or 1024 × 1528 pixels, preferably with a wide-aperture lens and fiber-optic light source. Since cellular metals exhibit heterogeneous deformation, the field of view should be optimized so that each unit cell can be mapped to approximately 50 pixels in each direction[14, 15].

The deformation evolution with strain from 2% to 5% are displayed as false plots of components of strain(Fig. 7). The incremental distortion at loadings between the start of non-linear response and the onset of the plateau reveals that localized deformation bands initiate at the onset of non-linearity having width about one cell's diameter. Within each band, there are cell-sized regions that exhibit strain levels about an order of magnitude larger than the applied strain. Outside the bands, the average strain is small and within the elastic range. The band normals are usually within 20° of the loading axis, but in some condition it reaches 40°. The principle strains reveal that the flow vectors are primarily in the loading direction, normal to the band plane. Moreover, the incremental distortion maps show new sets of collapse bands that form in regions neighboring previously formed bands.

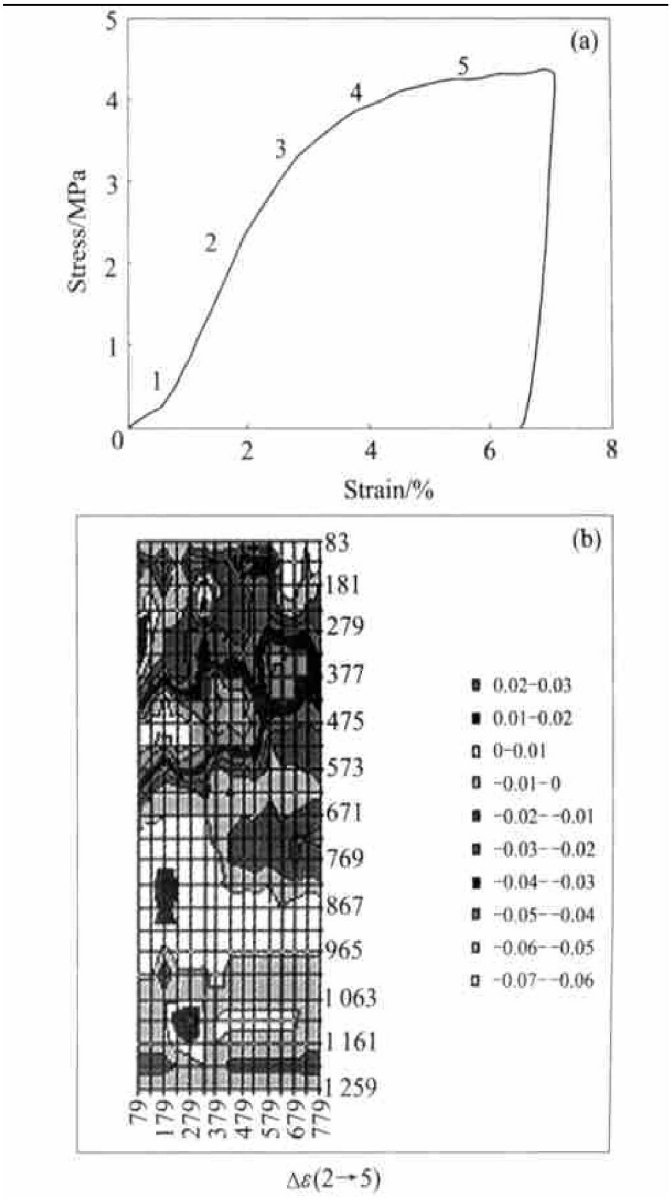

Fig. 7 Stress—strain curve(a) and surface map of incremental principal strains(b)

4 CONCLUSIONS

1) The cell size of foam with density of 0.37 mg/m^3 is distributed in the range of 0.5 - 4.0 mm. The cell size of foam with density of 0.33 mg/m^3 is distributed in the range of 0.5 - 5.0 mm. The cell wall thickness of both types is 0.1 - 0.3 mm.

2) The closed-cell aluminum foam almost belongs to isotropic one, with a variation of ±15% in elastic modulus and yield strength in longitudinal and transverse direction.

3) Under compressive loading, foam materials show inhomogeneous macroscopic deformation. The site of the onset of local plastic deformation depends on the cell structure. The shape of cell is more important than size in determining the yielding susceptibility of the cells.

4) At early stage of deformation, the deformation is localized in narrow bands having width of one cell's diameter, and outside the bands the cell still remains

the original shape. The cells within bands experience large permanent deformation. The band normals are usually within 20° of the loading axis.

REFERENCES

[1] Baumeister J, Banhart J, Weber M. Aluminum foams for transport industry[J]. Materials & Design, 1997(4): 217-223.

[2] Banhart J. Manufacture, characterization and application of cellular metals and metal foams[J]. Progress in Materials Science, 2001, 46: 559-632.

[3] Claar T D, Yu C-Y, Banhart J, et al. Ultra-light-weight aluminum foam materials for automotive applications[J]. International Journal of Powder Metallurgy, 2000, 36: 61-73.

[4] Körner C, Singer R F. Processing of metal foams-challenges and opportunities[J]. Advanced Eng Mater, 2000, 2: 159-165.

[5] Gergely V, Degischer H P, Clyne B. Aluminum foam for automotive applications[J]. Advanced Eng Mater, 2002, 2: 175-178.

[6] Lorenzi L, Fossat E, Todaro E. Aluminum foam applications for impact energy absorbing structures[A]. Proceedings of the Applications for Aluminum in Vehicle Design[C]. Detroit, Michigan, USA, 1997, 23.

[7] Claar T D, Irick V, Adkins J. Multifunctionality of closed-cell aluminum foams[A]. TMS 2002[C]. Seattle, Washington, USA, 2002.

[8] Jahn R, Sherman A M. Perspectives on high-volume automotive applications of light-weight cellular metals and structures[A]. TMS 2002[C]. Seattle, Washington, USA, 2002.

[9] LIU Pei-Sheng, YU Bing, HU Ar-min, et al. Development in applications of porous metals[J]. Trans Nonferrous Met Soc China, 2001, 11(5): 629-638.

[10] Ashby M F, Fleck N A. Metal Foams: A Design Guide[M]. Oxford, UK: Butterworth-Heinemann, 2000. 40, 77.

[11] Olurin O B, Fleck N A, Ashby M F. Deformation and fracture of aluminum foams[J]. Mater Sci Eng A, 2000, A291: 136-146.

[12] Bart-Smith H, Evans A G, Spyeck D J, et al. Compressive deformation and yielding mechanisms in cellular Al alloys determined using X-ray tomography and surface strain mapping[J]. Acta Mater, 1998, 46: 3583-3592.

[13] Sugimura Y, Bart-Smith H, Evans A G, et al. On the mechanical performance of closed cell Al alloy foams[J]. Acta Mater, 1997, 45: 5245-5259.

[14] Markaki A E, Clyne T W. The effect of cell wall microstructure on the deformation and fracture of aluminum-based foams[J]. Acta Mater, 2001, 49: 1677-1686.

[15] Bastawros A F, Manuis R. Use of digital image analysis software to measure non-uniform deformation in cellular aluminum alloys[J]. Exp Tech, 1998, 22, 35-37.

(Edited by YANG Bing)